Shape of the fluidity gradient in the plasma membrane of living HeLa cells

James M. Collins,[1,*] Raymond N. Dominey,[†] and W. McLean Grogan[*]

Department of Biochemistry and Molecular Biophysics,[*] Medical College of Virginia, Campus of Virginia Commonwealth University, Richmond, VA 23298-0614, and Department of Chemistry,[†] University of Richmond, Richmond, VA 23173

Abstract The shape of the fluidity gradient of the outer hemileaflet of the plasma membrane of living HeLa cells was determined using a series of n-(9-anthroyloxy) fatty acid probes where n = 2, 3, 6, 7, 9, 10, 11, 12, and 16. Fluorescence uptake and steady-state anisotropy values were obtained with a flow cytometer capable of continuous recording over time of vertical and horizontal emission intensities, and of the output of these intensities as calculated anisotropy values. The fluorescence uptake of all of the membrane probes was rapid up to about 15 min. The magnitudes of the uptake of fluorescence were, for the n-(9-anthroyloxy) series, in the order $2 > 3 > 6 > 7 > 9 > 10 > 11 = 12 = 16$. Anisotropy values were constant from 5 to 30 min after addition of the various probes, and the magnitudes were in the order $7 > 6 > 9 = 10 > 2 = 3 > 11 > 12 > 16$, indicative of the shape of the fluidity gradient. No differences were noted between the values obtained with 12-(9-anthroyloxy) stearic acid and 12- (9-anthroyloxy) oleate. The kinetics of anisotropy exhibited by those probes with the anthroyloxy group in positions deeper than 9, where initially higher values declined until equilibrium was reached, were probably indicative of an energy barrier at the approximate depth sensed by 7AS. —**Collins, J. M., R. N. Dominey, and W. M. Grogan.** Shape of the fluidity gradient in the plasma membrane of living HeLa cells. *J. Lipid Res.* 1990. **31:** 261–270.

Supplementary key words anthroyloxy fatty acids • fluorescence anisotropy • flow cytometry • membrane fluidity

Singer and Nicolson's fluid mosaic model (1) of biological membranes visualizes proteins embedded in a fluid, two-dimensional sea of lipids. The plate tectonics model, a modification proposed by Jain (2), recognizes that there are a number of ordered regions or discreet domains, which are in motion with respect to each other and separated by more disordered regions that are also in motion (3, 4). From these descriptions and a consideration of the anisotropic motion of the acyl chains of the phospholipid molecules about an axis perpendicular to the membrane surface has come the idea of a bulk membrane fluidity. The term fluidity includes the concept of motion, determined by the rate of movement of the acyl chains. The rotational motion of fluorescent probes can easily be assessed by fluorescence anisotropy, keeping in mind that such measurements are direct measures of probe motion and only indirectly a measure of the freedom of motion of the surrounding acyl chains.

Anthroyloxy fatty acid probes

Various membrane probes can penetrate and become accommodated by the acyl chains of the lipid bilayer. However, one of the paramount problems in the use of membrane probes as indicators of fluidity is the determination of their location in the lipid bilayer. For example, while it is fairly well documented that 1-[4-(trimethylammonio)phenyl]-6-phenyl-1,3,5-hexatriene (TMA-DPH) anchors in the outer hemileaflet with the charged group in the aqueous phase (5, 6), uncharged 1,6-diphenyl-1,3,5-hexatriene, or DPH, is able to localize at several positions (7). Waggoner and Stryer (8) proposed the use of a fluorescent fatty acid derivative, 12-(9-anthroyloxy) stearic acid (12AS) as a means of insertion of a probe at a defined transverse position in the bilayer. Other analogs in the n-(9-anthroyloxy) stearate series were synthesized, 2AS, 6AS, and 9AS, and two members of an n-(9-anthroyloxy) palmitic acid series, 2AP and 16AP (9–11), making it possible to examine the fluidity at different depths in lipid bilayers.

Interpretation of fluidity studies with the anthroyloxy probes assumes that the motional characteristics of the anthroyloxy group are independent of position on the alkane chain. Tilley, Thulborn, and Sawyer (12) used fluorescence polarization measurements to determine that, in liquid paraffin, the motions of 6AS, 9AS, and 12AS were indistinguishable, whereas 2AS had a slightly

Abbreviations: TMA-DPH, 1-[4-(trimethylammonio)phenyl]-6-phenyl-1,3,5-hexatriene; DPH, 1,6-diphenyl-1,3,5-hexatriene; nAS, n-(9-anthroyloxy)stearic acid; nAP, n-(9-anthroyloxy)palmitic acid; nAO, n-(9-anthroyloxy)oleic acid; DMSO, dimethylsulfoxide; PBS, phosphate-buffered saline; POPC, 1-palmitoyl-2-oleoyl-phosphatidylcholine; nAU, n-(9-anthroyloxy)undecanoic acid.

[1]To whom reprint requests should be addressed.

greater polarization predictive of more restricted motion (due to interaction, possibly hydrogen bonding, between the ester and carboxyl groups) and 16AP had much lower polarization values, predictive of considerably greater freedom of motion (due to its lack of steric hindrance from being located at the end of the alkane chain). Vincent et al. (13) confirmed these conclusions using time-resolved anisotropy studies.

Location of anthroyloxy fatty acid probes

It is well accepted that the AS probes locate at different depths in lipid bilayers (14). For example, the aqueous quenching of anthroyloxy fluorescence in isolated beef mitochondria was in the order 2>6>9>12>16, whereas with a quencher that partitions into the lipid phase near the bilayer center the order was reversed (15). With spin-labeled fatty acids as paramagnetic quenchers, the decreasing order of quenching with respect to alkyl chain position, n, was always 2, 6, 9, 12, and 16 in model lipid bilayers (16). Therefore, the most reasonable interpretation of various studies of model lipid bilayers is that the anthroyloxy probes appear to locate in a graded series of depths from the surface to the center of the lipid bilayer.

Fluidity gradients with anthroyloxy fatty acid probes

A gradient of continuously increasing fluidity from the surface to the center of the bilayer, in the order 2>6 (or 7)>9>12>16, has been observed using fluorescence polarization measurements with DPPC model membrane systems (12, 13, 17) and isolated mitochondria (15). Therefore, in model systems composed of saturated fatty acids, the anthroyloxy fatty acid probes have reflected a continuously increasing gradient of fluidity from the surface to the bilayer center.

It is important to note that the shape of the fluidity gradient in model bilayer systems is different when unsaturated fatty acids or cholesterol are included. The shape can be changed from continuous to discontinuous (6>9>2>12) by the inclusion of an unsaturated fatty acid such as oleic (18, 19), or of 20 mol % cholesterol (17). Cholesterol inclusion also caused greater polarization values, indicating decreased fluidity in the outer hemileaflet (17).

It is well known that the complex plasma membranes of living cells contain substantial amounts of unsaturated fatty acids and cholesterol, as well as protein, and that the composition varies widely with respect to cholesterol content, phospholipid class, and chain heterogeneity. In erythrocyte ghosts (11) and in red blood cells (20), a continuous, very shallow gradient (order of 6 = 9>12>16) was observed. Moreover, in *Escherichia coli* plasma membranes, a continuous gradient (order of 2>3>6>9>12>16) was found (21). The fluidities reported by 6AS and 7AS relative to one another have not been determined with any system, model or biological. Although different cell types exhibit a range of anisotropy values as measured by one or a few probes and those values can be modified by various physiological, pharmacological, or pathological perturbations (22), nothing is known about the variation of the entire fluidity gradient as a function of cell type. Moreover, there are no reports addressing effects on the shape of the fluidity gradient by normal processes such as dietary variations, cell differentiation, cell proliferation, cell cycle phases, and aging; agents such as hormones, drugs, and toxins, which are known to interact with membranes; or pathological causes such as cancer. There has been a single report concerning the shape of the fluidity gradient in living, nucleated cells (18) in which four anthroyloxy fatty acid probes were used to determine that the order of fluorescence polarization in mouse thymocytes was 6>2 = 9>12.

Recently, we reported that the fluidity near the surface of the plasma membrane of a homogeneous model cell system, HeLa cells, was less than that nearer the center of the bilayer, using a flow cytometer to measure the anisotropy of 1-[4-(trimethylammonio)phenyl]-6-phenyl-1,3,5-hexatriene (TMA-DPH) and 12AS (23). In the present study we report measurement of the shape of the entire fluidity gradient using a series of n-(9-anthroyloxy) fatty acids at probe concentrations 10–25 times less than those generally used with static fluorometry, with a flow cytometric technique that selectively analyzes viable, living cells as a continuous function of time. This report represents a first step in our plan to measure the fluidity gradients of a variety of cell types and to attempt to determine the effects of membrane composition on the shapes of the fluidity gradients.

EXPERIMENTAL PROCEDURES

Cell culture

HeLa S3 cells (0.5×10^6/ml) were maintained in spinner culture at 37°C. Cells were fed every 48 h with Joklik's modified Eagle's minimal essential medium containing 10% fetal calf serum and 1.25% fungizone, and routinely monitored for mycoplasma as previously described (24). As fungizone is a membrane-active agent, cells to be used in experiments were grown on media lacking fungizone for at least two cell generations before harvest.

Cell staining

A series of membrane probes, 2-(9-anthroyloxy) stearate (2AS), 2-(9-anthroyloxy) palmitate (2AP), 3-(9-anthroyloxy) stearate (3AS), 6-(9-anthroyloxy) stearate (6AS), 7-(9-anthroyloxy) stearate (7AS), 9-(9-anthroyloxy) stearate (9AS), 10-(9-anthroyloxy) stearate (10AS),

11-(9-anthroyloxy) undecanoate (11AU), 12-(9-anthroyloxy) stearate (12AS), 12-(9-anthroyloxy) oleate (12AO), and 16-(9-anthroyloxy) palmitate (16AP), were purchased from Molecular Probes Inc. Eugene, OR. These probes were dissolved in DMSO at 50 μM, diluted into PBS to 0.5 μM, and sonicated at the lowest setting for 1 min just before use. HeLa cells were washed and resuspended in phosphate-buffered saline (PBS: 136.9 mM NaCl, 8.1 mM Na_2HPO_4, 2.68 mM KCl, 1.47 mM KH_2PO_4, 0.68 mM $CaCl_2$, 0.24 mM $MgSO_4$) at 2 × 10^6 cells/ml for flow cytometry. Under these conditions greater than 95% of the cells remain viable for over an hour as judged by the ability to exclude propidium iodide and retain fluorescein diacetate. Dual-angle light scatter (forward and 90°) analysis was employed and gates were set to discriminate against the nonviable cells. Equal volumes of cells and stain dispersals at 25°C were mixed and gently vortexed for 15 sec just prior to measurements. In some experiments, the cells were incubated with stain for 30 min; in others, measurements were begun 1 min after addition of stain.

Flow cytometry

The EPICS 753 flow cytometer supplied by Coulter Electronics, Hialeah, FL, has been described (23). Optical path of the EPICS 753 is as follows. The laser beam is polarized vertically (parallel) with respect to the sample stream, and is tuned to the 351 and 364 nm lines. Optical elements placed 90° to the sample stream collect and shape the light resulting from intersection of the cells with the laser beam, and direct it along the optical train where it first encounters an RE400 dichroic mirror which deflects 20% of the light 90° to a photomultiplier for measurement of 90° light scatter. A long pass interference filter, 418 nm, was used to remove scattered laser light from the transmitted (80%) beam. The correct orientation of sheet polarizers obtained from Coulter Electronics was determined with a spectrophotometer and they were mounted in front of two other photomultipliers (PMT) designated as intensity vertical (parallel), I_V, and intensity horizontal (perpendicular), I_H. A 50% beam splitter (Corion) permits about half of the light beam to pass through to the I_V PMT with the remainder deflected 90° to the I_HPMT (we detected no changes in final anisotropy values, after balancing, when the I_V and I_H PMTs were switched). For convenience, an analog function board outputs anisotropy in channel numbers, calculated as, $r_{channel} = (I_V - I_H)/(I_V + 2I_H)$.

Calibration

We used the convenient means of calibration of the $r_{channel}$ anisotropy values using the LED (light emitting diode) in the flow cytometer as previously described (25). Anisotropy values output by the analog function board were obtained from a series of constant I_V and varying I_H PMT voltages, and compared with (intrinsic) anisotropy values manually calculated from the outputs of the I_V and I_H PMTs. The regression formula from the calibration curve was $r_{calculated} = 0.003843 (r_{channel} + 0.0125$, and the correlation coefficient for linearity was 0.997. It should be stressed that anisotropy values conveniently obtained in this manner are identical to those manually calculated from the I_V and I_H intensities $(r = (I_V - I_H)/(I_V + 2I_H)$.

Balancing

Balancing of the I_V and I_H PMTs was performed with the stained cells being studied. A UV half-wave retarder plate (Karl Lambrecht, 355 nm) was placed in a mount obtained from Coulter Electronics and aligned at the horizontal (perpendicular) position with respect to the plane of polarization of the laser beam in order to achieve depolarization of the observed fluorescence at each of the PMTs (26). The voltage was adjusted on the I_H PMT so that the intensity was equal to that of the I_V PMT, resulting in an anisotropy output that was centered at channel 0. This was checked by integrating the anisotropy output from channel 0 to channel 1, which should be equal and approximate one-half of the number of cells.

Anisotropy

For nonkinetic measurement of anisotropy, the half-wave retarder is aligned vertical (parallel) to the polarization of the laser beam and the anisotropy is recorded. The anisotropy values in channels obtained with HeLa cells stained for 30 min with 1 μM DPH, were r (44.1), I_V (106.6), and I_H (63.9). This corresponds to an anisotropy value of 0.182 whether calculated from the calibration curve formula $[r = 0.003843 (r_{channel} + 0.0125]$, or from $r = (I_V - I_H)/(I_V + 2I_H)$. The anisotropy of Hoechst 33258-stained HeLa was 0.29 ± 0.004 (SEM), similar to the value reported by Jovin (27) of 0.28 with Friend erythroleukemia cells. These compare favorably with the value 0.32 ± 0.009 (SEM), previously obtained by us for Hoechst 33258-stained HeLa using an SLM subnanosecond fluorometer (4800C series, SLM Instruments, Urbana, IL) (23), and the value 0.32, measured in Hoechst-stained Friend erythroleukemia cells by Jovin (27) with a similar static fluorometer. In other experiments designed to determine variability of cells stained for 30 min with 1 μM DPH, anistropy values of 0.182 ± 0.008 (SEM) were obtained, similar to the value of 0.179 reported by Shinitzky and Barenholz (22) for fibroblasts. Thus, anisotropy measurements with the flow cytometer under the conditions described above appear to be adequate.

Kinetic analysis

In addition to simultaneous, multiparametric analysis of forward and 90° light scatter, I_V and I_H, as described above, time was used as a correlated parameter by means of the flow cytometer clock. Thus, the data from four PMTs, and time were stored as five-dimensional matrices containing the number of cells corresponding to each of the five measured parameters in a manner preserving the association of events. These data can then be displayed as contour plots (see Fig. 2A) of fluorescence or anisotropy versus time, or as 3-D plots (see Fig. 2B) with cell number being the third parameter.

Data analysis

The kinetic data were analyzed with the flow cytometric computer program, "Cytology" (Coulter Electronics). This permits selection of time intervals of data displayed in the form of contour plots, followed by projection of the anisotropy distribution, which creates a single parameter representation of anisotropy versus channel number for that time interval, and finally, calculation of the means of the projected anisotropy distributions, expressed in channel numbers. Channel number values are converted into intrinsic anisotropy values as described above under Calibration.

For further calculations, statistics, and preliminary graphic analysis, the data were imported into the computer program "Lotus 123" (Lotus Development Corporation). Data from this program were imported into "Slidewrite Plus" (Advanced Graphics Software, Inc., Sunnyvale, CA) for presentation graphs. Molecular models were constructed and dimensions in nm were determined with the computer program "Alchemy" (Tripos Associates, Inc., St. Louis, MO).

Photobleaching minimalization

Photobleaching under conditions of ordinary laboratory lighting can be a serious source of artifact with cells stained with fluorescence probes, as discussed by Bently et al. (28). When cells were stained for 30 min with 0.25 μM probe and subsequently allowed to stand uncovered with the room's lights on at 25°C for 30 min, the fluorescence of TMA-DPH-stained cells decreased to about 40% of the starting value, and that of 6AS-stained cells decreased to about 31%. When the same experiment was performed in the dark, the fluorescence of TMA-DPH-stained cells decreased to about 96%, and 6AS-stained cells decreased to about 88%, with no change in anisotropy values. Therefore, all subsequent experiments were performed with the room lights extinguished and the samples covered with foil.

RESULTS

Relative position of anthroyloxy fatty acids

The fatty acid probes used in this study, a series of n-(9-anthroyloxy) stearates, where n = 2 (2AS), 3 (3AS), 6 (6AS), 7 (7AS), 9 (9AS), 10 (10AS), and 12 (12AS), as well as 11-(9-anthroyloxy) undecanoate (11AU), 12-(9-anthroyloxy) oleate (12AO), and 16-(9-anthroyloxy) palmitate (16AP), are illustrated in **Fig. 1** as computer-drawn CPK models, along with cholesterol (Ch) and 1-palmitoyl-2-oleoyl-phosphatidylcholine (POPC) for orientation. The distance spanned by POPC is about 2.8 nm from the phosphoryl moiety to the terminal methyl residue, placing the center of a phospholipid bilayer at a depth of about 3 nm. Aligning the carboxyl of an n-(9-anthroyloxy) fatty acid with the phosphate of POPC,

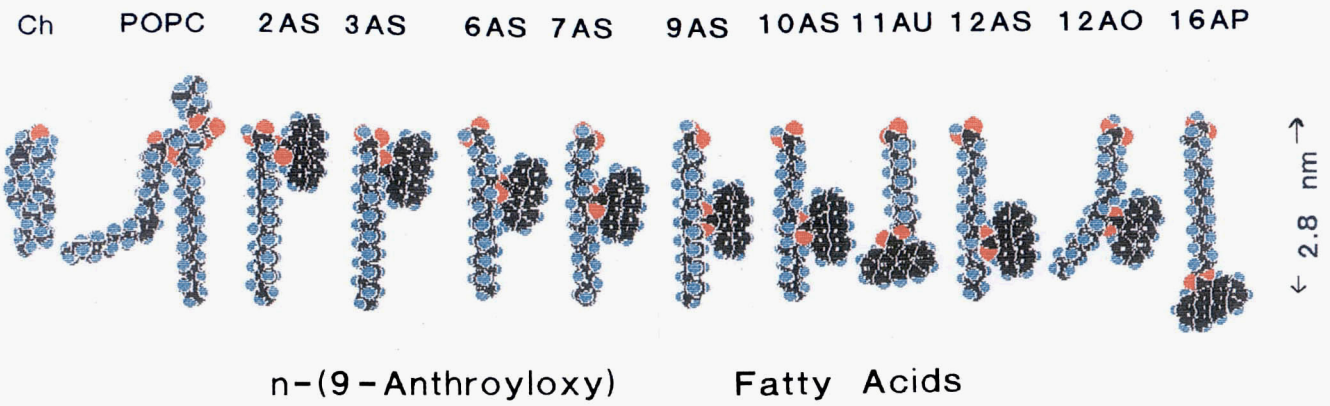

Fig. 1. CPK models of a series of n-(9-anthroyloxy) fatty acid probes. The CPK space-filling models were generated by the program "Alchemy," which was also used to determine intramolecular distances in nm. Illustrated from left to right are: cholesterol, 1-palmitoyl-2-oleoyl-phosphatidylcholine (POPC), which spans a distance of about 2.8 nm from the phosphoryl linkage to the end, and the various n-(9-anthroyloxy) probes. The relative alignments shown are consistent with previous observations placing the anthracene ring of 2AP level with the ester linkages of the acyl chains of the phospholipids (29), and those placing part of the anthracene ring in contact with water (11). The bend shown in POPC is solely to illustrate the position of the 9,10 *cis* double bond, not to suggest that this structure exists in membranes as well as in crystals.

gives a rough measure of the depth that the anthroyloxy ester group would be expected to penetrate. For the AS probes, the distances from the carboxyls to the centers of the anthroyloxy groups are: 0.24 nm (2AS and 2AP), 0.326 nm (3AS), 0.73 nm (6AS), 0.85 nm (7AS), 1.09 nm (9AS), 1.21 nm (10AS), 1.33 nm (11AU), 1.45 nm (12AS), 1.44 nm (12AO), and 2.36 nm (16AP). These relative alignments are consistent with the quenching data of Podo and Blasie (29), and that of Thulborn and Sawyer (11).

Single-parameter flow cytometric anisotropy distributions of 30-min stained cells

The means of the anisotropy distributions of cells stained for 30 min with various anthroyloxy fatty acid probes were determined. The decreasing order of the mean anisotropy values, in channel numbers and intrinsic values ± SEM, respectively, were for all probes: 7AS (45.7, 0.188 ± 0.004), 6AS (44.6, 0.184 ± 0.003), 9AS (41.5, 0.172 ± 0.002), 10AS (41.2, 0.171 ± 0.002), 2AS (39.9, 0.166 ± 0.004), 2AP (39.9, 0.166 ± 0.003), 3AS (39.7, 0.165 ± 0.005), 11AU (37.9, 0.158 ± 0.003), 12AS (35.0, 0.147 ± 0.004, 12AO (35.1, 0.147 ± 0.006), and 16AP (31.1, 0.132 ± 0.002). Such measurements with cells that have been exposed to a probe for a period of 30 min reflect the overall bulk fluidity of cells, but not necessarily the fluidity of the plasma membrane. The initial equilibration of a probe with the membrane is a process that may occur over a period of a few minutes. After longer times of exposure there may be subsequent equilibrations with other more fluid environments of the cell, such as the interior, by means of probe redistribution (23).

Flow cytometric kinetics of probe uptake and anisotropy

The continuous uptake kinetics of fluorescence and of anisotropy after the addition of 6AS to HeLa cells is presented in **Fig. 2**. The fluorescence kinetics over a period of time from 1 to 30 min are shown as a contour plot in Fig. 2A. The anisotropy kinetics over a period of time from 1 to 30 min are shown as a 3-D plot in Fig. 2B, with cell number being the third parameter, for illustrative purposes. Selected intervals of time (analogous to taking "slices") of contour plots are projected by the computer program; these now have the appearance of single parameter distributions, with Gaussian shapes. From these, means in channel numbers are calculated and converted to fluorescence or anisotropy values, as described in Experimental Procedures. All subsequent data are reported as the means of the distributions derived in this way.

As can be seen, fluorescence rapidly increases up to 5 min and is essentially constant after 10 min (Fig. 2A), while anisotropy is fairly constant for 30 min with this probe (Fig. 2B).

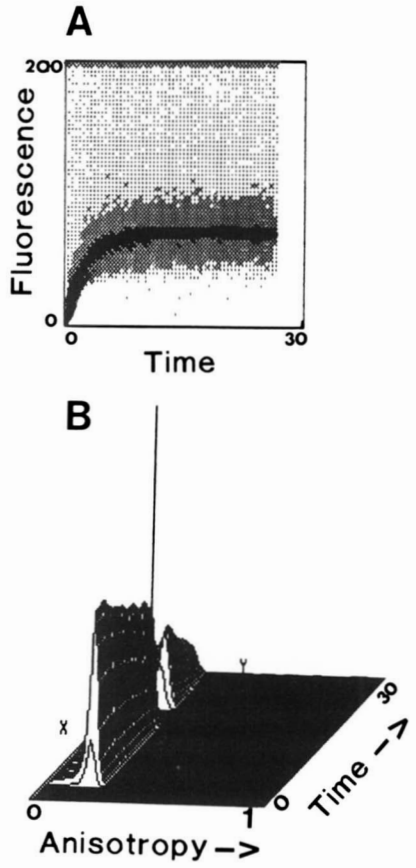

Fig. 2. Flow cytometric fluorescence and anisotropy distributions using time as a parameter. Probes were added to HeLa at 0.25 μM and analysis was begun after 1 min, as described in Experimental Procedures. The axis designated Time on the figures refers to a 30-min period. Panel A: a contour plot of fluorescence versus time. Contour plots are representations of 3D surfaces where the level of two measured parameters per cell (in this case fluorescence intensity and time) defines the location of the cells. The dot density is the "elevation" at that point and defines the frequency of the cells. Panel B: three-dimensional plot where the Z-axis indicates the relative numbers of cells at the coordinates of anisotropy and time. A "slice" representing time from 20 to 23 min was removed from the data as an aid to visual perception.

Determination of nonperturbing concentrations of probe

A serious source of artifact in fluorescence anisotropy measurements with living cells is the use of high (i.e, perturbing) concentrations of probes. A sign of excessive probe is an observed decrease in anisotropy while fluorescence intensity due to probe uptake continues to increase. Bouchy, Donner, and Andre (30) have shown that this decrease in anisotropy can be indicative of translocation into more fluid environments inside the cells. As expected, the kinetics of fluorescence increase (i.e., probe uptake) were displaced toward higher fluorescence as the concentration of 6AS was increased from 0.25 μM to 3μM (**Fig. 3A**). Over the same time period (30 min), the anisotropy values were constant with 0.25 and 0.5 μM, but

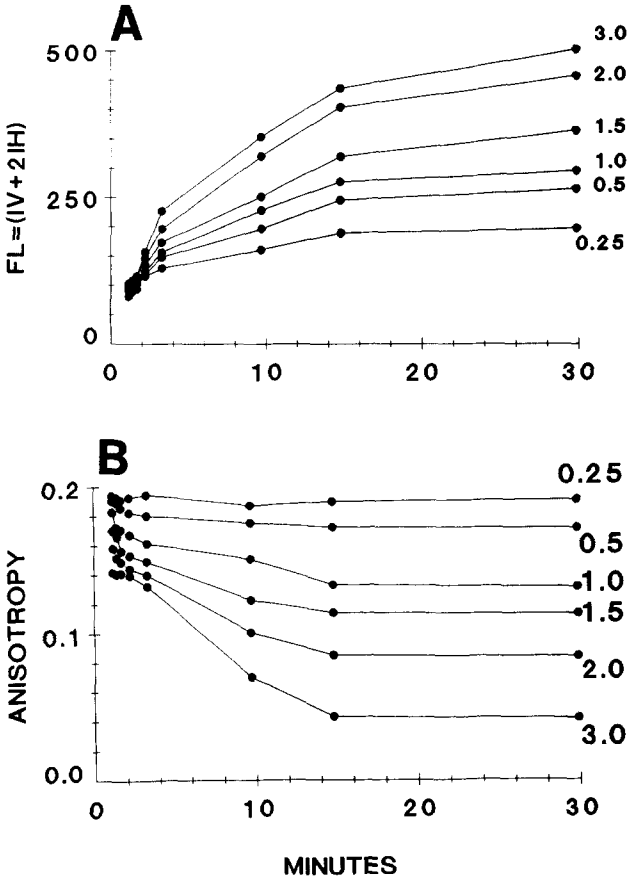

Fig. 3. Kinetics of uptake and anisotropy with various concentrations of 6AS. The probe 6-(9-anthroyloxy) stearate was added to HeLa in 0.25, 0.5, 1, 1.5, 2, and 3 μM concentrations as indicated on the figures, and analysis was performed as described in the legend to Fig. 2. Means were calculated from projected data at selected time points as described in Experimental Procedures. Panel A: fluorescence; panel B: anisotropy.

declined at greater concentrations (Fig. 3B). When concentrations of 0.2, 0.15, and 0.1 μM were used, the fluorescence decreased as expected, but the resulting anisotropy values were virtually identical to those obtained with 0.25 μM (data not shown), indicating that concentrations of 0.25 μM and below are nonperturbing. Accordingly, all subsequent experiments were performed with 0.25 μM concentrations of probes.

Kinetics of fluorescence uptake and anisotropy of a series of anthroyloxy probes

The maximum levels of fluorescence uptake of probes with n = 2–10 decreased with increasing anthroyloxy group position, that is, the order was: $2>3>6>7>9>10$ (**Fig. 4A**). In contrast, derivatives with n greater than 10, all reached essentially the same maxima (Fig. 4B). As expected, the fluorescence uptake of 2AP (Fig. 4B) was essentially identical to that of 2AS (**Fig. 5A**). Subtle differences are apparent in the uptake of the probes with increasing n values; it took about 15 min for 2, 3, 6, and 7 to reach essentially constant fluorescence, and about 30 min for 9, 10, 11, 12, and 16 (Figs. 4A and 4B).

The anisotropy values of all of the probes reached constancy after about 5 min, with little subsequent decrease even after 30 min (Figs. 4C and 4D). Differences were apparent in the behavior of the probes over the period from 1 to 5 min. Probes with the anthroyloxy group at positions 2, 3, 6, and 7 had initial (1 min) values that remained essentially constant over the next 5 min (Fig. 4C). However, with probes having the anthroyloxy group at positions, $n>7$, the initial values decreased over the next 5 min. The magnitudes of these differences between initial and 5-min values were dependent on anthroyloxy location in the order: $9<10 = 11 = 12<16$ (Figs. 4C and 4D). It can also be noted that the curves representative of the anisotropy kinetics of 12AS and 12AO, stearate and oleate, respectively, are identical. Although the bend in the oleate chain due to the *cis* double bond places the terminal methyl group nearer the surface than would be the case with a stearic acid chain containing the same number of methylene residues, the anthroyloxy of 12AO is quasi-laterally displaced and not significantly nearer the surface (see Fig. 1), hence the similarity in anisotropic behavior between 12AO and 12AS should not be surprising.

Shape of the fluidity gradient in the HeLa cell plasma membrane

The data of Figs. 4C and 4D were analyzed for the anisotropy values at discreet times after addition of probe, and are expressed with respect to position of the anthroyloxy group (Fig. 5). The bold arrow in Fig. 5A indicates times 5.2 min and 29.1 min, for which the data are almost superimposable. There are two conclusions that can be drawn from these data. First, anthroyloxy derivatives with positions greater than 7 require longer times for equilibration than those at lesser positions, with the times required seemingly a function of position (Fig. 5A). Two, the shape of the fluidity gradient, indicated by the shape of the anisotropy gradient at 5 min or longer, followed the order, with respect to n-position of the probes, of $7<6<9 = 10<2 = 3 = 11<12<16$ (Fig. 5A, 5-min). Thus, the HeLa plasma membrane appears to be most rigid at a depth sensed by 7AS and most fluid at depths sensed by 16AP (Fig. 5).

DISCUSSION

Steady-state anisotropy measurements by means of flow cytometry offer several advantages over static fluorometry for membrane studies with living cells. In general, the sensitivity of fluorescence techniques allows

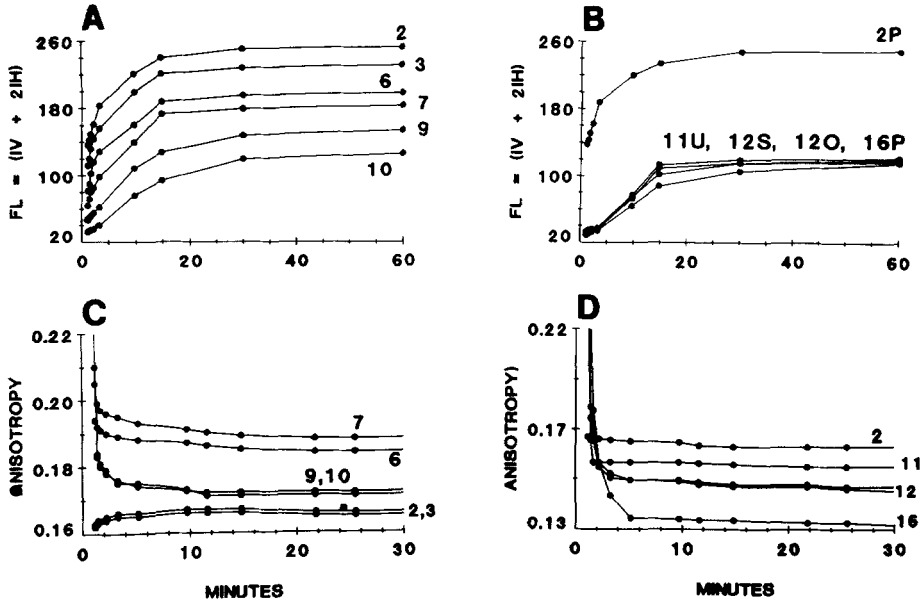

Fig. 4. Kinetics of fluorescence uptake and anisotropy. A series of probes were added at 0.25 μM and analysis was begun after 1 min, as described in the legend to Fig. 3. The probes used are indicated on the figures, and refer to: panel A: fluorescence of: 2, 3, 6, 7, 9, and 10AS; panel B: fluorescence of: 2AP, 11AU, 12AS, 12AO, and 16AP; panel C: anisotropy of: 2, 3, 6, 7, 9, and 10AS; and panel D: anisotropy of: 2AP, 11AU, 12AS, 12AO, and 16AP.

the use of low probe concentrations where perturbations are not severe, and , in particular, the intense laser beam of the flow cytometer permitted us to easily measure the anisotropy of cells labeled with 0.25 μM concentrations of anthroyloxy probes within 1 min after uptake. Whereas a static fluorometer measures all fluorescence in the light path, a flow cytometer measures only the fluorescent pulse from a cell intersecting the laser beam and is insensitive to any background fluorescence of unbound probe molecules, which are evenly dispersed through the sample stream regardless of their aggregation state. The flow cytometer's clock permits continuous recording for kinetic experiments. Photobleaching effects of the sample are practically nonexistent, in spite of the intense laser beam, as a cell is illuminated (and analyzed) only once for a few microseconds. "Parasitic" light scatter due to the simultaneous illumination of hundreds of thousands of cells in a sample, which is extremely difficult to remove with probes of low fluorescence emission intensities (31), such as the AS series, is avoided by single cell analysis. Something not possible with static fluorometry is the use of dual-angle light scatter profiles for selective analysis of only those cells of interest. By this means, subpopulations of damaged cells within a homogeneous cell culture can be ignored and cells that become nonviable over the time course of kinetic experiments will also be ignored. Lastly, populations of cells in heterogeneous mixtures such as blood, marrow, liver, kidney, spleen, etc., can be resolved without using lengthy separation procedures (Collins, J. M., and W. M. Grogan, unpublished observations).

There has been one previous flow cytometric study using anthroyloxy fatty acid probes (32). Although the issue

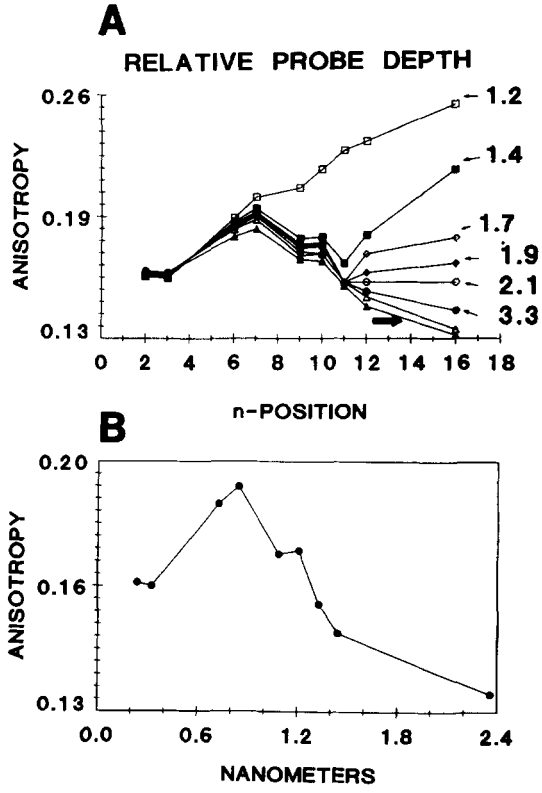

Fig. 5. Shape of the fluidity gradient. The data are taken from Figs. 4C and 4D and are expressed as anisotropy versus relative n-position of the various probes. The SEM were similar to those noted in the text, for 30-min stained cells. Panel A: anisotropy versus position number of probe, at times indicated on the figures, which were, 1.2, 1.4, 1.7, 1.9, 3.3, 5.1, and 29.1 min with the broad arrow at the bottom of the figure indicative of 5.1, and 29.1 min. Panel B: anisotropy versus distance in nm of the anthroyloxy group from the carboxyl group of the various probes (from Fig. 1), at time = 5.1 min.

addressed was membrane fluidity changes upon differentiation of mouse F9 cells, (where no differences were observed with 2AS, 6AS, 9AS, and 12AS, but, surprisingly, differences were noted with TMA-DPH), comparisons can be made between their data and ours. Specifically, their reported I_V/I_H values were, in order, 6>9>2>12, which is consistent with our findings. Conversion of their data into anisotropy yields values, for the same order, of, 0.133, 0.155, 0.138, and 0.094, which are considerably lower than our values for 30-min stained HeLa, of 0.184, 0.172, 0.166, and 0.147 (Fig. 2). However, the differences between the values with HeLa and those with F9 cells are most likely due to differences in cell type as we have noted lower values for these probes with HL-60 cells (Collins, J. M., and W. M. Grogan, unpublished observations).

There is no doubt that anthroyloxy fatty acids if used in sufficiently high concentrations will perturb lipid bilayers. However, with HeLa (data not shown) and lymphocytes (Collins, J. M., and W. M. Grogan, unpublished observations) mixed with low (0.25 μM) concentrations of anthroyloxy fatty acids, we have observed no changes in the dual light-scatter pattern (a decrease in light-scatter intensity is generally indicative of membrane damage resulting in changes in refractive index due to loss of the permeability barrier). Cells mixed with increasing concentrations of 6AS, from 1 to 3 μM, exhibited behavior consistent with increasing membrane perturbation, that is, a continuously declining anisotropy over a period of 30 min (Fig. 3B). On the other hand, cells mixed with low amounts, 0.25 μM, exhibited a fairly constant anisotropy over a period of 30 min (Fig. 3B), behavior consistent with scant perturbation of the plasma membrane. Observation by means of visual microscopy with high levels of these probes revealed that first the outer periphery of the cells (presumably the plasma membrane) become fluorescent, then after about 15 sec, the interior became fluorescent, indicative of translocation to the interior (data not shown). However, such behavior was not noted when 0.25 μM probe was used (it should be noted that it is extremely difficult to see fluorescence with this low level of probe). After 5 min, interior fluorescence was just barely detectable with most of the fluorescence located in the outer periphery (data not shown). The interior only became (slightly) fluorescent after 30 min exposure (data not shown). Thus, while we cannot rule out that some translocation occurred, we believe it to have made only a minor contribution to the measured anisotropy values, and feel confident in the interpretations derived from those values obtained over the first few minutes after the addition of the probes.

Interestingly, the magnitudes of fluorescence uptake of the series of anthroyloxy probes, were, in decreasing order, 2>3>6>7>9>10>11>12>16 (Figs. 4A and 4B). This observation is entirely consistent with those of Haigh et al. (33), who observed that the order of uptake by phosphatidylcholine liposomes was 2AP>6AS>9AS>12AS. Haigh et al. (33) interpreted their data as due to a decrease in the number of binding sites as the anthroyloxy group was moved further away from the carboxyl group of the probes. This in turn is likely to be due to an increased size of the probe micelles or aggregates as n increases; current theories about the effect of the overall shape of amphiphiles on the size of their micelles or aggregates predict that an increase in the radii of curvature will result as the anthroyloxy group is moved further away from the carboxyl group (34).

Anisotropy declined from 1 to 5 min with those probes with the anthroyloxy group located at positions deeper than C_7 along the alkyl chain, whereas it did not decline with those probes with this group at 2, 3, 6, or 7 (Figs. 4C and 4D). Cadenhead et al. (10) have inferred from conductance and capacitance data with model membranes that these fatty acids can assume folded or extended shapes depending on location of the anthroyloxy group, and that folded structures would assume erect conformations during penetration of the plasma membrane, which could theoretically cause an initial high, then declining anisotropy. However, the times involved for simple conformational changes would be orders of magnitudes shorter that those observed for the declines in anisotropy (Figs. 4C and 4D), hence conformational changes of the probes are not a plausible explanation. The simplest interpretation consistent with the existance of a fluidity minimum at the position reported by 7AS is that this least fluid region constitutes an energy barrier, through which large molecules such as membrane proteins, or in this case those probes with the bulky anthroyloxy group "deeper" than position 7, would face (relative) difficulty in penetrating. Such a viscosity barrier has been noted for phosphatidylcholine liposomes (18). We envision that as the anthroyloxy group of the deeper probes intially encounters this barrier, it has much less freedom of motion and exhibits relatively high initial anisotropy values, which later decrease as the group penetrates through the barrier on to localization in more fluid membrane regions. The data of Fig. 4A are consistent with such an energy barrier, as the times required for the anisotropy values to reach a state of equilibrium are about 1.2 min for the n = 2, 3, 6, and 7 members, envisioned as the time for positioning into the membrane above the barrier, and about 1.4 min for 9 and 10, envisioned as the time for locating in closer proximity to the barrier. Finally, it takes about 1.7 min, 3.3 min, and 5 min for 11, 12, and 16, respectively, envisioned as the time for complete penetration through the barrier (Fig. 4A). It should be noted that interaction of the anthroyloxy group with other polar groups in the membrane, such as ester linkages,

might also delay penetration to deeper regions.

The most significant aspect of our study is the determination of the shape of the fluidity gradient in the HeLa plasma membrane. If the anisotropy values represent a fluidity gradient, as studies with model membranes suggest (11–13, 15, 17, 19–21), then the shape of the gradient is indicated by the relationship of the anisotropy values versus anthroyloxy position (Fig. 5). The least fluid region is reported by 7AS (Fig. 5). Next would be, in order, those regions reported by 6AS, 9AS and 10AS, 2AS, 2AP and 3AS, 11AU, 12AS, 12AO, and finally, 16AP. These data should be interpreted with caution, as Tilley et al. (12) have suggested that changes in polarization may reflect changes in the anisotropy of motion, as well as rate of motion. However, the shape of this gradient would be only slightly modified if corrections were made for the slightly more hindered motion of 2AS (and by inference, 2AP), and the considerable greater freedom of motion of 16AP (and by inference, 11AU) (12). Whether expressed as anisotropy, as shown in Fig. 5, or as polarization, $(I_V - I_H)/(I_V + I_H)$, (data not shown), this shape is different from the only other report with living cells, which were mouse thymocytes (18). Those cells exhibited a maximum at the C_6 depth of the probes, and all four values were considerably less than those we observed (i.e., conversion of their polarization values yields for the AS probes, 2, 6, 9, and 12, anisotropy values of 0.067, 0.091, 0.083, and 0.064, compared to our values of 0.166, 0.184, 0.172, and 0.147, see Fig. 5).

The shape of the fluidity gradient of HeLa cells (Fig. 5) is not nearly as shallow as that observed with model systems or isolated membranes, and only tentative inferences regarding the effects of membrane components on the shape in HeLa can be made at this time. In plasma membranes from HeLa cells grown under conditions similar to ours, 59% of the fatty acids are unsaturated, i.e., 16:1 (4%), 18:1 (23%), 20:4 (26%), 24:1 (2%), and 22:6 (4%) (35). In model systems, the presence of 18:1 gave a maximum anisotropy with 6AS and it was proposed that the anthroyloxy group interacted with the 18:1 double bond (17, 19). However, HeLa plasma membranes also contain substantial amounts (26%) of 20:4, and this may also have a significant contribution.

HeLa plasma membranes also contain considerable cholesterol, about 48 mol% cholesterol:phospholipid (36). In saturated model systems, the addition of cholesterol caused maximum anisotropy with 6AS (17). In its extended configuration, cholesterol spans 1.6 nm from the hydroxyl group to the hydrocarbon side chain (Fig. 1). Although the potential for interaction of cholesterol with the anthroyloxy group is present, no reason for the maximum anisotropy with 7AS in HeLa instead of 6AS or 9AS is apparent. However, it has long been known that the insertion of cholesterol into model phospholipid bilayers increases the rigidity to a depth of approximately 6–9 carbons, while increasing fluidity in deeper regions (37), and this general observation is consistent with our findings with living HeLa cells.

Thus, at present, the relationship between membrane composition and the shape of the fluidity gradient in living cells is not clear, and studies wherein the fatty acid and/or cholesterol contents are modified are required. Lastly we expect that different cells (with their differing membrane compositions) will exhibit different fluidity gradients. In preliminary studies with white blood cells we have observed that not only are the shapes different, but that the maximum anisotropies are different, i.e., the probes that had greatest anisotropy were, for neutrophils, 6AS, for lymphocytes, 7AS, and for macrophages, 9AS (Collins, J. M., and W. M. Grogan, preliminary observations).

The skilled and cheerful technical assistance of Annie K. Chu and Frances H. White is greatly appreciated. This investigation was supported in part by NIH grants nos. CA-24158 (JMC), and HD-13019 (WMG).

Manuscript received 19 May 1989 and in revised form 18 August 1989.

REFERENCES

1. Singer, S. J., and G. L. Nicholson. 1972. The fluid mosaic model of the structure of cell membranes. *Science.* **175:** 720–731.
2. Jain, W. K. 1983. Nonrandom lateral organization in bilayers and biomembranes. *In* Membrane Fluidity in Biology. Vol. I. R. C. Aloia, editor. Academic Press, New York. 1–37.
3. Yechiel, E., and M. Eididin. 1987. Micrometer-scale domains in fibroblast plasma membranes. *J. Cell Biol.* **105:** 755–760.
4. Treistman, S. N., M. M. Moynihan, and D. E. Wolf. 1987. Influence of alcohols, temperature, and region on the mobility of lipids in neuronal membrane. *Biochim. Biophys. Acta.* **898:** 109–120.
5. Fisher, P. B., D. Schachter, and R. E. Abbott. 1984. Membrane lipid dynamics in human promyelocytic leukemia cells sensitive and resistant to 12-O-tetradecanoylphorbol-13-acetate induction of differentiation. *Cancer Res.* **44:** 5550–5554.
6. Petty, H. R., C. D. Niebylski, and J. W. Francis. 1987. Influence of immune complexes on macrophage membrane fluidity: a nanosecond fluorescence anisotropy study. *Biochemisty.* **26:** 6314–6318.
7. Mulders, F., H. Van Langen, G. Van Ginkel, and Y. K. Levine. 1986. The static and dynamic behaviour of fluorescent probe molecules in lipid bilayers. *Biochim. Biophys. Acta.* **859:** 209–218.
8. Waggoner, A. S., and L. Stryer. 1970. Fluorescent probes of biological membranes. *Proc. Natl. Acad. Sci. USA.* **67:** 579–589.
9. Barratt, M. D., R. A. Bradley, R. B. Leslie, C. G. Morgan, and G. K. Radda. 1974. The interaction of apoprotein from porcine high-density lipoprotein with dimyristoyl phosphatidylcholine. *Eur. J. Biochem.* **48:** 595–601.

10. Cadenhead, D. A., B. M. J. Kellner, K. Jacobson, and D. Papahadjopoulos. 1977. Fluorescent probes in model membranes. I. Anthroyl fatty acid derivatives in monolayers and liposomes of dipalmitoylphosphatidylcholine. *Biochemistry.* **16:** 5386–5392.
11. Thulborn, K. R., and W. H. Sawyer. 1978. Properties and the locations of a set of fluorescent probes sensitive to the fluidity gradient of the lipid bilayer. *Biochim. Biophys. Acta.* **511:** 125–140.
12. Tilley, L., K. R. Thulborn, and W. H. Sawyer. 1979. An assessment of the fluidity gradient of the lipid bilayer as determined by a set of n-(9-anthroyloxy) fatty acids (n = 2, 6, 9, 12, 16). *J. Biol. Chem.* **254:** 2592–2594.
13. Vincent, M., B. de Foresta, J. Gallay, and A. Alfsen. 1982. Nanosecond fluorescence anisotropy decays of n-(9-anthroyloxy) fatty acids in dipalmitoylphosphatidylcholine vesicles with regard to isotropic solvents. *Biochemistry.* **21:** 708–716.
14. Blatt, E., and W. H. Sawyer. 1985. Depth-dependent fluorescent quenching in micelles and membranes. *Biochim. Biophys. Acta.* **822:** 43–62.
15. Chatelier, R. C., and W. H. Sawyer. 1985. The transverse organisation of ubiquinones in mitochondrial membranes as determined fluorescence quenching. Evidence for a two-site model. *Eur. Biophys. J.* **11:** 179–185.
16. Blatt, E., R. C. Chatelier, and W. H. Sawyer. 1984. The transverse location of fluorophores in lipid bilayers and micelles as determined by fluorescence quenching techniques. *Photochem. Photobiol.* **39:** 477–483.
17. Thulborn, K. R., L. M. Tilley, and W. H. Sawyer, and E. Treloar. 1979. The use of n-(9-anthroyloxy) fatty acids to determine fluidity and polarity gradients in phospholipid bilayers. *Biochim. Biophys. Acta.* **558:** 166–178.
18. Thulborn, K. R., F. E. Treloar, and W. H. Sawyer. 1978. A microviscosity barrier in the lipid bilayer due to the presence of phospholipids containing unsaturated acyl chains. *Biochem. Biophys. Res. Commun.* **81:** 42–49.
19. Vincent, M., and J. Gallay. 1984. Time-resolved anisotropy study of effect of a *cis* double bond on structure of lecithin and cholesterol-lecithin bilayers using n-(9-anthroyloxy) fatty acids as probes. *Biochemistry.* **23:** 6514–6522.
20. Howard, R. J., and W. H. Sawyer. 1980. Changes in the membrane microviscosity of mouse red blood cells infected with *Plasmodium berghei* detected using n-(9-anthroyloxy) fatty acid fluorescent probes. *J. Parasitol.* **80:** 331–342.
21. Dombek, K. M., and L. O. Ingram. 1984. Effects of ethanol on the *Escherichia coli* plasma membrane. *J. Bacteriol.* **157:** 233–239.
22. Shinitzky, M., and Y. Barenholz. 1978. Fluidity parameters of lipid regions determined by fluorescence polarization. *Biochim. Biophys. Acta.* **515:** 367–394.
23. Collins, J. M., and W. M. Grogan. 1989. A comparison between flow cytometry and fluorometry for the measurement of membrane fluidity parameters. *Cytometry.* **10:** 44–49.
24. Collins, J. M. 1978. Rates of DNA synthesis during the S-phase of HeLa cells. *J. Biol. Chem.* **253:** 8570–8577.
25. Fox, M. H., and T. M. Delohery. 1987. Membrane fluidity measured by fluorescence polarization using an EPICS V cell sorter. *Cytometry.* **8:** 20–25.
26. Pinkel, D., M. Epstein, R. Udkoff, and A. Norman. 1978. Fluorescence polarimeter for flow cytometry. *Rev. Sci. Instrum.* **49:** 905–912.
27. Jovin, T. M. 1979. Fluorescence polarization and energy transfer: theory and application. *In* Flow Cytometry and Sorting. M. R. Melamed, P. F. Mullaney, and M. L. Mendelsohn, editors. John Wiley and Sons, New York. 137–165.
28. Bentley, K. L., L. K. Thompson, R. J. Klebe, and P. M. Horowitz. 1985. Fluorescence polarization: a general method for measuring ligand binding and membrane microviscosity. *BioTechniques.* **3:** 356–366.
29. Podo, F., and J. K. Blasie. 1977. Nuclear magnetic resonance studies of lecithin bimolecular leaflets with incorporated fluorescent probes. *Proc. Natl. Acad. Sci. USA.* **74:** 1032–1036.
30. Bouchy, M., M. Donner, and J. C. Andre. 1981. Evolution of fluorescence polarization of 1,6-diphenyl-1,3,5-hexatriene (DPH) during the labeling of living cells. *Exp. Cell Res.* **133:** 39–46.
31. Teale, F. W. J. 1969. Fluorescence depolarization by light-scattering in turbid solutions. *Photochem. Photobiol.* **10:** 363–374.
32. Schaap, G. H., J. E. de Jong, and J. F. Jongkind. 1984. Fluorescence polarization of six membrane probes in embryonal carcinoma cells after differentiation as measured on a FACS II cell sorter. *Cytometry.* **5:** 188–193.
33. Haigh, E. A., K. R. Thulborn, L. W. Nichol, and W. H. Sawyer. 1978. Uptake of n-((9-anthroyloxy) fatty acid fluorescent probes into lipid bilayers. *Aust. J. Biol. Sci.* **31:** 447–457.
34. Evans, D. F., and B. W. Ninham. 1986. Molecular forces in the self-organization of amphiphiles. *J. Phys. Chem.* **90:** 226–234.
35. Keegan, R., P. A. Wilce, E. Ruczkal-Pietrzak, and B. C. Shanley. 1983. Effect of ethanol on cholesterol and phospholipid composition of HeLa cells. *Biochem. Biophys. Res. Commun.* **114:** 985–990.
36. Konings, A. W. T., and A. C. C. Ruifrok. 1985. Role of membrane lipids and membranes fluidity in thermosensitivity and thermotolerance of mammalian cells. *Radiat. Res.* **102:** 86–98.
37. Tanford, C. 1973. The Hydrophobic Effect: Formation of Micelles and Biological Membranes. John Wiley & Sons, New York.